International Journal of Heat and Mass Transfer 90 (2015) 406–417

Contents lists available at ScienceDirect

International Journal of Heat and Mass Transfer

journal homepage: www.elsevier.com/locate/ijhmt

Computer simulation of radio frequency selective heating of insects in soybeans

Zhi Huang [a], Long Chen [a], Shaojin Wang [a,b,*]

[a] College of Mechanical and Electronic Engineering, Northwest A&F University, Yangling, Shaanxi 712100, China
[b] Department of Biological Systems Engineering, Washington State University, Pullman, WA 99164-6120, USA

ARTICLE INFO

Article history:
Received 2 February 2015
Received in revised form 23 June 2015
Accepted 23 June 2015

Keywords:
Computer simulation
Insect control
RF energy
Differential heating
Soybean

ABSTRACT

Radio frequency (RF) treatments have potential as alternatives to chemical fumigation for disinfesting legumes. This study was conducted to investigate the feasibility of RF selective heating of insect larvae in 3 kg soybeans packed in a rectangular plastic container ($30 \times 22 \times 6$ cm^3) using a 6 kW, 27.12 MHz RF heating system. A finite element based computer simulation program-COMSOL was used to solve the coupled electromagnetic and heat transfer equations for developing a simulation model. Indianmeal moth larvae were selected as the target insect for experimental validation of the simulation results. Simulated and experimental temperatures of insects and soybeans after 6 min RF heating were compared in top, middle, and bottom layers within the container. Both results showed that insect larvae were differentially heated with 5.9–6.6 °C higher than host soybeans when RF heated from 25 to 50 °C. These results revealed that the heating rate of insects was 1.4 times greater than that of soybeans. The validated simulation results demonstrated that placing the insect on the cold spot of each layer, or horizontally, and large insect size may cause less selective heating within the insect bodies. Dielectric properties of insects may also influence the preferential heating patterns. The selective heating of insects in soybeans may provide potential benefits in developing practical RF treatments to ensure reliable control of insect pests without adverse effects on product quality.

1. Introduction

Soybeans are one of important legumes in current international market, with an annual production of 241 million metric tons in 2012 and 91 million tons were exported in 2011 by the 9 leading countries for a value of US$51 million [1]. Preservation of soybeans for long-term storage has always been a challenge due to infestation by various insects. The major pest for concern is the Indianmeal moth, *Plodia interpunctella* and other internal pests are the cowpea weevil, *Callosobruchus maculatus*, and red flour beetle, *Tribolium castaneum*, respectively. These insects reduce the quality of products and promote mold growth or toxin production, which may create technical barriers to export and even pose a serious threat to consumer health. The total postharvest product losses due to insect damages are conservatively estimated to be between 10% and 40% worldwide [2]. The most common method for postharvest insect control in soybeans is chemical fumigation with methyl bromide (MeBr), which is a broad spectrum pesticide with low cost and high effectiveness. However, the major problem of MeBr fumigation is the negative impact on environment due to depleting ozone layer [3]. With actions taken by the Montreal Protocol, MeBr is no longer available to the legumes industry for postharvest phytosanitary treatments. In addition, because of the rapidly growing market for organic soybeans, there is an urgent need to find environmentally friendly and effective alternatives to chemical fumigation for soybeans.

Radio frequency (RF) technology with a frequency of 1–300 MHz has long been proposed as a potential alternative to chemical fumigation and applied for control of different insects for various agricultural products [4,5]. Recently, RF treatment protocols have been developed to effectively control cowpea weevil in legumes (chickpea, lentil and green pea) with acceptable product quality [6,7]. RF heating relies on vibration of polar molecules and movement of ions, which result in heat generation. The interaction of RF electromagnetic field with any material depends on its dielectric properties [8]. It has been established that the insect has higher dielectric properties than the host material they infest, which would lead to faster heating of the insect when compared with the treated samples [9–13]. Insects might reach a lethal

* Corresponding author at: College of Mechanical and Electronic Engineering, Northwest A&F University, Yangling, Shaanxi 712100, China. Tel.: +86 2987092391; fax: +86 2987091737.
E-mail address: shaojinwang@nwsuaf.edu.cn (S. Wang).

http://dx.doi.org/10.1016/j.ijheatmasstransfer.2015.06.071
0017-9310/

Nomenclature

A	surface area (m^2)
c_p	heat capacity (J/kg °C)
d	diameter (m)
E	electric field intensity (V/m)
E_{is}	ratio of the insect-to-soybean electric field intensity
f	frequency (Hz)
h_c	heat transfer coefficient at the sample surface(W/m^2 °C)
I_a	measured anode current (A)
k	thermal conductivity (W/m °C)
Q	power density generated by electric field (W/m^3)
t	time (s)
T	sample temperature (°C)
$\partial T/\partial t$	increase rate of temperature (°C/s)
V	electric potential (V)
V	volume (m^3)
SD	standard deviation
ε	permittivity (F/m)
ε_0	free space permittivity (F/m)
ε'	dielectric constant (dimensionless)
ε''	dielectric loss factor (dimensionless)
∇	gradient operator
ρ	density (kg/m^3)

Subscripts

i	insect
s	soybean

temperature while products would be heated to a lower temperature that does not cause quality loss [14–16]. Nelson and Charity firstly suggested that it would be possible to generate differential heating between rice weevil and winter wheat based on the measured dielectric properties in a frequency range of 10–100 MHz [17]. A theoretical analysis and experimental evidence showed that codling moth larvae were heated 1.4–1.7 times faster than walnut kernels at 27.12 MHz, but no preferential heating was observed at microwave frequencies of 915 MHz [13]. Wang et al. reported, based on direct measurements using model insects made of gellan gel and from theoretical predictions, that the mean temperature differences between model insects and almond kernels were 4.7 and 6.0 °C at heating rates of 5 and 10 °C/min, respectively [18]. Studies on electromagnetic interactions with the insect and products also showed that the insect-to-wheat power dissipation factor was between 5 and 31 depending upon insect-wheat mixture temperature (15–75 °C), and wheat moisture level (12–18% wet basis) at the test frequency of 27.12 MHz [19].

Computer simulation is a very effective tool for rapid, cost-effective, and flexible analyses, and providing an insight into the dielectric heating mechanism in food materials [20–23]. To help understand the complex RF dielectric heating process and analyze RF heating uniformity, simulation has previously been used in various food materials, such as dry soybeans [24], fresh fruits [25], mashed potato [26], meat [27], peanut butter [28], raisins [29] and wheat flour [30]. Zhu et al. simulated the top electrode voltage based on finite element method using COMSOL Multiphysics to predict the correlation between electrode voltages and electrical currents [31]. Ben-Lalli et al. developed a space-and-time dependent computer simulation model including convective heating and microwave heating (915 MHz) using commercially available finite element based software, COMSOL [32]. The model was then validated by comparing simulated and experimental temperature profiles inside date fruit and the results showed a realistic magnitude and information on insect survival rates under given treatment conditions and characteristics of dates and insects. Validated simulation models are very useful to analyze the different RF heating characteristics between insect pests and dry products, reduce adverse effects on product quality, and provide a greater throughput of product in a processing plant. There are few reports on the finite element simulation to show the differential heating of insects in host soybeans when subjected to an electromagnetic field.

The objectives of this study were to: (1) develop a computer simulation model for a 6 kW, 27.12 MHz RF system using commercial finite element software COMSOL, (2) validate the computer simulation model by comparing three-layer transient experimental temperature profiles in soybeans after 6 min RF heating, and (3) apply the validated computer simulation model to predict the effects of insect positions, orientations, dielectric properties, and sizes on the behavior of differential RF heating between insects and soybeans.

2. Materials and methods

2.1. Sample preparation

2.1.1. Dry soybeans

Seeds of soybean (Glycine mux L.) were obtained from a local wholesale market in Yangling, Shaanxi, China. The seeds were stored with mesh bags in a thermostatic and humidity (65% RH) controlled chamber (BSC-150, Shanghai BoXun Industrial & Commerce Co., Ltd., Shanghai, China) at the constant temperature (25 °C) prior to RF experiments. They were taken out from the chamber 4 h before experiment and kept at ambient room temperature (25 ± 1 °C) for equilibration.

2.1.2. Insects

Larvae of Indianmeal moth were obtained from the Entomological Institute, College of Plant Protection, Northwest A&F University, Yangling, China. Larvae were kept in a glass jar containing 200 g of dry soybeans. The jars were covered by a fine mesh cloth for air exchange, and maintained in a rearing room at 25 ± 1 °C, 65% RH, and a photoperiod of 16:8 (*L*:*D*) *h* with artificial light. Only actively moving Indianmeal moth larvae were used in RF treatments and the weight of each larva was about 0.04 ± 0.003 g. The length and diameter of Indianmeal moth larvae ranged from 10 to 13 mm and from 2.2 to 2.8 mm, respectively. These insect larvae were transferred from glass jars to plastic cups (500 ml) and left at room temperature for 4 h before treatments.

2.2. Material properties measurement

Different sample moisture content may change dielectric and thermal properties of materials, which would further influence the RF heating behavior [24]. So moisture content of soybeans was determined using the oven drying method. About 10 g of ground soybeans were placed in an aluminum dish and dried in an oven (DZX-6020B, Shanghai Nanrong Co. Ltd., Shanghai, China) at 120 °C for 12 h until a substantially constant weight was obtained. The average initial moisture content of dry soybeans was 6.18 ± 0.04% on wet basis (w.b.) together with that

(74.0% w.b.) of insect larvae reported in the literature [12]. The bulk density of dry soybeans at room temperature was measured by a basic volume method using a $30 \times 22 \times 6$ cm^3 plastic rectangular container and obtained to be 739 ± 3 kg/m^3 over three replicates. Thermal properties (thermal conductivity and specific heat) at a bulk density of 739 kg/m^3 were calculated by Deshpande's regression equations [33,34]. Thermal properties of the insect larvae were reported by Ben-Lalli et al. and Sahin and Sumnu with different measured components [32,35]. Dielectric properties of bulk soybeans and Indianmeal moth larvae at 27 MHz were obtained from Guo et al. and Wang et al., respectively [10,12]. Dielectric constant and loss factor of the samples increased with increasing moisture content. These data were subjected to linear regression analysis for using these properties in simulation model (Table 1). Dielectric and thermal properties of polypropylene container and air at room temperature (25 °C) were adapted from COMSOL material library [36].

2.3. Simulation model development

2.3.1. Physical model

A 6 kW, 27.12 MHz parallel electrodes, pilot scale free-running RF unit (COMBI 6-S, Strayfield International Limited, Wokingham, UK) was used in this research, with an area of 83×40 cm^2 for the top plate electrode and a larger bottom plate electrode (Fig. 1). In the RF cavity (2.98 m long, 1.09 m wide and 0.74 m high), about 3 kg dry soybeans were placed inside polypropylene plastic containers ($30 \times 22 \times 6$ cm^3) for RF treatment. RF power from the generator was fed in the middle of top electrode back side and proportional to the electrode gap by changing the top electrode position with the help of adjustable screws [31]. The product container was placed on the bottom (ground) electrode.

2.3.2. Governing equations

In existing RF applicators, RF wave lengths (~11 m) are usually longer compared to the RF applicator size. Therefore, the Maxwell's equation can be simplified to Laplace equation by neglecting the effect of magnetic field. Laplace equation is described by a quasi-static assumption [25]:

$$-\nabla \cdot ((2\pi f \varepsilon_0(\varepsilon'' + j\varepsilon'))\nabla V) = 0 \quad (1)$$

where f is the working frequency, ε_0 is the permittivity of the free space (8.86×10^{-12} F/m), ε'', ε' are the loss factor and dielectric constant of the treated material, $j = (-1)^{0.5}$, and V is the voltage between the two electrodes which related to the electric field ($E = -\nabla V$).

Since the voltage in the typical industrial-scale RF systems varies only 7% between standby to full load position [38], a constant electric potential can be assumed for top electrode of RF systems. The top electrode voltage was estimated by the following equation with the measured anode current (I_a) of 0.33 A [31]:

$$V = 11242 \times I_a + 2029.9 \quad (2)$$

The RF power conversion per unit volume Q in the dielectric material is given by:

$$Q(x, y, z, t) = 2\pi f \varepsilon_0 \varepsilon'' |E|^2 \quad (3)$$

where $Q(x, y, z, t)$ is the power density of treated material, and $|E|$ is the modulus of $E(x, y, z, t)$ field.

Temperature rise in the treated material can be calculated by the unsteady heat transfer equation given by [25]:

Table 1
Properties of Indianmeal moth, dry soybeans, polypropylene and air used for simulation.

Material properties	Indianmeal moth [32,35]	Dry soybeans	Aluminum [36]	Air [36]	Polypropylene [36]
Density ρ (kg/m^3)	1008	739	2700	1.2	900
Thermal conductivity k (W/m °C)	0.51	0.11 [33]	160	0.025	0.26
Heat capacity c_p (J/kg °C)	3450	1829 [34]	900	1200	1800
Dielectric constant	0.81 * T + 63.12 [12]	0.048 * T + 0.81 [10]	1	1	2.0 [37]
Loss factor	4.42 * T + 109.86 [12]	0.007 * T − 0.05 [10]	0	0	0.0023 [37]

T-temperature ($20 \leqslant T \leqslant 60$ °C).

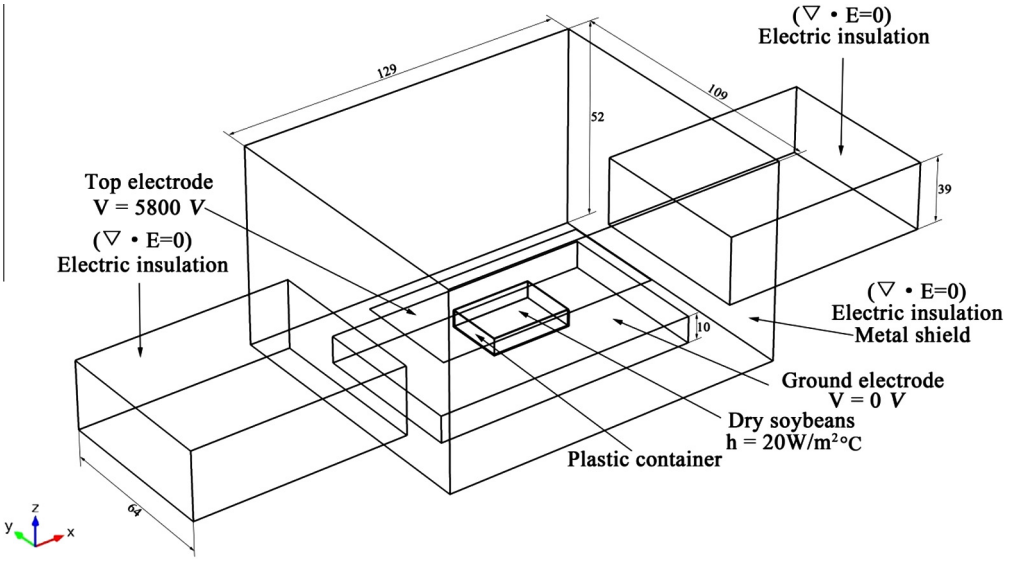

Fig. 1. Boundary and initial conditions for the RF system used in the computer simulation model (all dimensions are in cm).

$$\rho c_p \frac{\partial T}{\partial t} = k\nabla^2 T + Q(x,y,z,t) \quad (4)$$

When the insect and soybean samples were exposed to the same RF field, the soybean samples were heated uniformly over their element volumes and the geometry of insect larvae was characterized as a cylindrical shape. Heat transfer of soybean samples in the electromagnetic field can be described with the following non-linear heat diffusion equation:

$$\rho_s c_{ps}\left(\frac{\partial T}{\partial t}\right)_s = k_s\left(\frac{\partial^2 T}{\partial x^2}+\frac{\partial^2 T}{\partial y^2}+\frac{\partial^2 T}{\partial z^2}\right) + Q_s(x,y,z,t) \quad (5)$$

where ρ_s is the density of soybeans, c_{ps} is the heat capacity of soybeans, $(\partial T/\partial t)_s$ is the temperature increase rate of soybeans, k_s is the thermal conductivity of soybeans, and $Q_s(x, y, z, t)$ is the RF heat generation in soybeans.

The significant heat transfer may occur between insects and soybeans because of the relatively small size of the insect body when compared to soybean samples. Heat convection across the contact area between the insect and surrounding soybeans was assumed to be negligible since 3 kg of dry soybeans placed in the rectangular container were assumed as a whole. The heat balance equation of insect larvae was controlled by both heat conduction (k_i) and heat generation (Q_i) with the treated material, as follows [13,32]:

$$\rho_i c_{pi} V_i\left(\frac{\partial T}{\partial t}\right)_i = k_i A_i\left(\frac{\partial^2 T}{\partial x^2}+\frac{\partial^2 T}{\partial y^2}+\frac{\partial^2 T}{\partial z^2}\right) + Q_i(x,y,z,t)V_i \quad (6)$$

where ρ_i is the density of insect, c_{pi} is the specific heat of insect, $(\partial T/\partial t)_i$ is the temperature increase rate of insect, k_i is the thermal conductivity of insect, $Q_i(x, y, z, t)$ is the RF heat generation in insect, V_i is the volume of insect, and A_i is the surface area of insect.

The absorption of RF energy propagating through the material depends on the square of the electric field intensity, the electrical and physical characteristics of the treated material. The heating time (t) and frequency (f) are identical under the same RF treatment, but the electric field intensity in different materials is theoretically different [19]. In Eqs. (3) and (4), all the quantities can be measured accurately except $E(x, y, z, t)$ in and around the soybean samples and the insect bodies. Accurate calculation of field intensities in soybeans and insects is probably impossible, but some insight can be obtained by considering mathematically amenable models. To examine the relative electric field intensities in the insect (E_i) and soybeans (E_s), a theoretical model was developed on the basis of interaction of electromagnetic waves with multi-phase materials as following [19]:

$$E_i = E_s\left(\frac{3\varepsilon_s}{2\varepsilon_s+\varepsilon_i}\right) \quad (7)$$

where ε_i is the relative complex permittivity of the insect, ε_s is the relative complex permittivity of soybeans, E_i is the electric field within insect bodies, and E_s is the electric field within soybeans.

As can be seen from Eq. (7), when $\varepsilon_i >> \varepsilon_s$, the electric field intensity was almost same between insects and the host materials in microwave and RF heating [13,32]. In this study, to analyze the electric field distribution of insects under different conditions, Eq. (7) can be shown as:

$$E_{is} = \frac{E_i}{E_s} = 3\left(\frac{1}{2+\varepsilon_i/\varepsilon_s}\right) \quad (8)$$

where E_{is} is the ratio of E-fields per unit volume in the insect relative to that in soybeans medium.

2.3.3. Initial and boundary conditions

The whole geometry, thermal, and electrical boundary conditions of the computer simulation model is illustrated in Fig. 1. Electrode gap between the top and bottom electrode was fixed at 12 cm to achieve the suitable heating rate (4–6 °C/min) of dry soybeans [6,24]. All metallic shield were set as electrical insulation ($\nabla \cdot E = 0$). The upper electrode is maintained at a certain potential V_0, and the bottom electrode is maintained at the ground condition ($V = 0$). The electric potential on the top electrode (83×40 cm^2) was considered as 5800 V based on the measured anode current in Eq. (2). Heat loss due to airflow was modeled by specifying the convective heat transfer coefficient at the surface of the treated material. Initial temperatures of all cases of simulation were set as the ambient temperature (25 °C).

$$-k\nabla T = h_c(T - T_a) \quad (9)$$

where $h_c = 20$ W/(m^2 °C) is the convection heat transfer coefficient over the sample surface, $T_a = 25$ °C is the temperature of the air inside the RF cavity.

2.3.4. Simulation procedure

A numerical solution has been carried out using COMSOL Multiphysics 4.3a (COMSOL Multiphysics, CnTech Co., Ltd., Wuhan, China), a finite element method based software. The simulations have been performed by a Dell workstation, equipped with two Intel Xeon CPUs, at 3.10 GHz, with 8 GB of RAM, running under Windows 7 64 bit operating system. The built-in module (Joule heating module) was used to model the RF heating process, which combined both electromagnetic heating and heat transfer phenomena. For solving time-dependent problems, COMSOL uses a solver that is an implicit time-stepping scheme: at each time step, it solves a possibly nonlinear system of equations (COMSOL 4.3a User Guide). The optimal meshing type was obtained when the predicted temperature difference between the two sequential sets of mesh was less than 0.1% [30]. Relative tolerance and absolute tolerance were set to 0.01 and 0.001, initial and maximum time step were 0.001 and 0.1 s, respectively.

2.4. Model validation

2.4.1. Experimental procedure

To validate the developed computer simulation model, a plastic container filled with 3 kg of dry soybeans was placed on the bottom electrode in the center of RF cavity and heated by RF energy. The target average temperature for complete kill of insect pests in soybeans without quality degradation was estimated to be 50 °C for 2 min, based on the thermal-death kinetics of Indianmeal moth [39,40]. To ensure 100% insect mortality within the whole container of soybeans, the insect was placed on the center of each layer (cold spot). A fiber optical sensor (HQ-FTS-D120, Xi'an HeQi Opo-Electronic Technology Co., LTD, Shaanxi, China) was inserted through the polystyrene foam board to top layer center (cold spot) of soybeans to obtain the temperature–time history [24,29]. The heating time needed for the cold spot from ambient temperature (25 °C) to 50 °C was recorded. When the cold spot reached 50 °C, the sample was taken out immediately to take thermal image. The obtained temperature profiles were further used to validate the computer simulation model. All tests were replicated 3 times.

2.4.2. Temperature acquisition

When conducting experiments, 3 kg dry soybeans filled the container were horizontally divided into three layers (2, 4, and 6 cm from the container bottom) and separated by two thin gauzes with mesh opening of 1 mm [24]. A plastic foam board ($l = 29$ cm, $w = 21$ cm, $h = 2$ cm) made from polystyrene was used to cover on

the top of the container. Two holes (with distance of 1.5 cm) at the center of the board were drilled through the polystyrene foam sheet to allow fiber optical sensors to pass through [28]. Three fiber optical sensors (1, 2, 3 or 4, 5, 6) with an accuracy of ±1 °C were fixed through each hole (d = 5 mm), and fastened at three different vertical positions (1.4, 3.4, and 5.4 cm from the container bottom). Head of the fiber optical sensors (1, 2, and 3) were fixed in the middle of the cylinder-shaped ($12H \times 2.5D$ mm^2) insects (insect body positioned vertically) with scotch tape (width of 6 mm) to avoid loss of body fluid. All together, the board had 6 fiber optical sensors labeled in Fig. 2, which calibrated by using ice-water mixture and boiling water before experiment. Six fiber optical sensors were connected to a data acquisition system (FTS-P104, Xi'an HeQi Opo-Electronic Technology Co., LTD, Shaanxi, China) and temperatures were recorded at 1 s intervals. Fiber optical sensors placed at six typical positions (at three different layers) were used to monitor the temperature changes inside the samples. An infrared camera (DM63-S, DaLi Science and Technology Co., LTD, Zhejiang, China) with an accuracy of ±2 °C was used for mapping the surface temperatures of soybeans in top, middle, and bottom layers after the sample container was taken out from the heating cavity. The thermal digital infrared camera was first calibrated against a thin thermocouple thermometer (HH-25TC, Type-T, OMEGA Engineering Inc., Stamford, Connecticut, USA) with an accuracy of ±0.5 °C and 0.9 s response time. Based on the calibration, we selected 0.94 for the emissivity of the soybeans surface. The whole temperature measurement procedure was completed within 20 s. The experiments were replicated three times.

2.5. Model applications

2.5.1. Simulation results with different insect positions

After validation, the computer simulation model was used to study the temperature distribution of multiple insect positions at

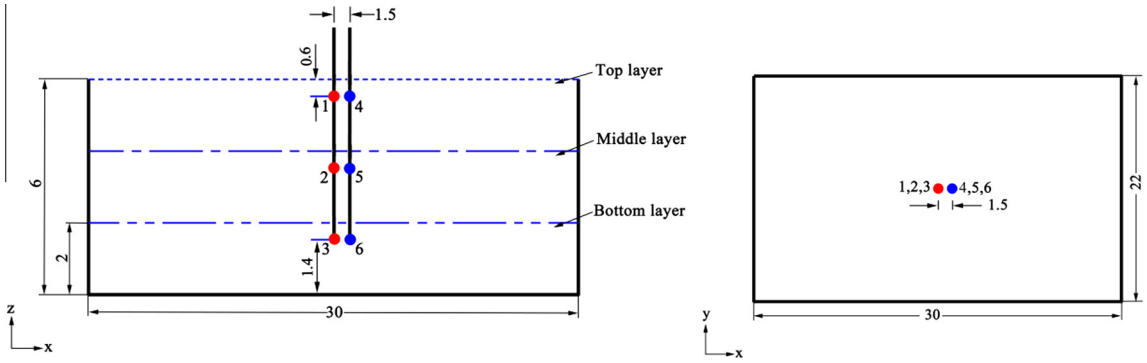

Fig. 2. Dimensions and locations of the plastic container and six fiber-optical sensors (with labeled locations) for measuring temperature distributions of cylinder-shaped ($12H \times 2.5D$ mm^2) insects (1, 2, and 3) and dry soybeans (4, 5, and 6) in each layer inside the rectangular container during RF treatments (all dimensions are in cm).

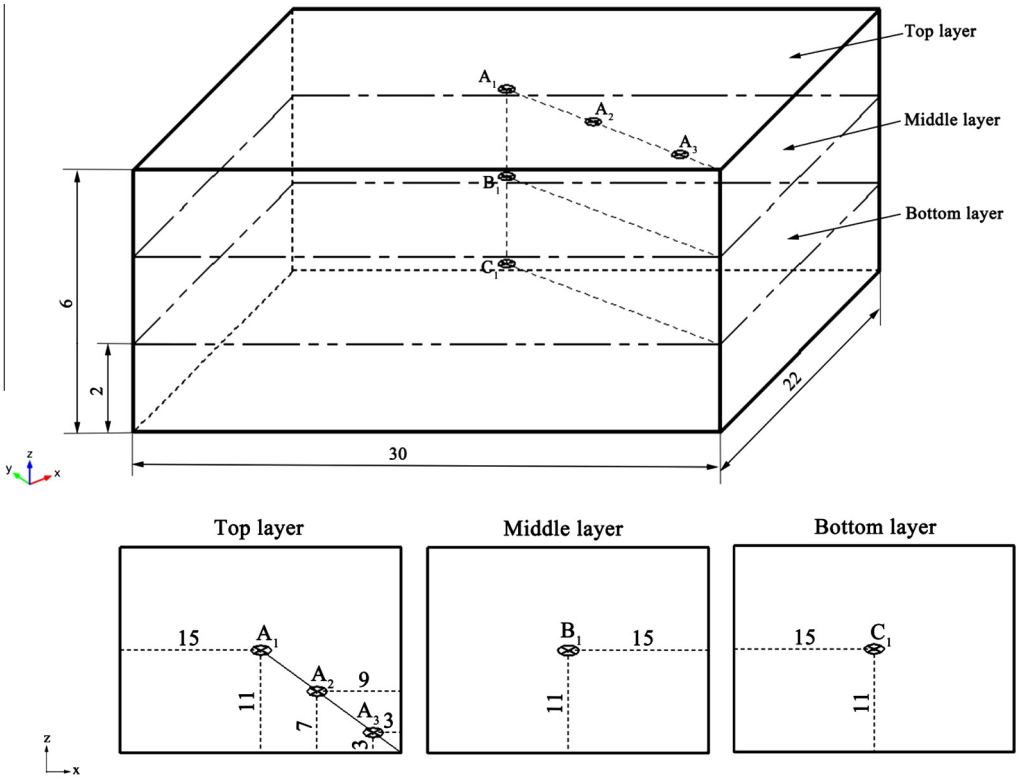

Fig. 3. Different positions of insects at the center part for each layer (A_1, B_1, and C_1) and three horizontal positions at the top surface layer (A_1, A_2, and A_3) after 6 min RF heating with insect body positioned vertically, electrode gap of 12 cm, and initial temperature of 25 °C (all dimensions are in cm).

treated soybeans in the RF cavity. The model considered three horizontal positions in each layer (A_1, A_2, and A_3 in the top layer; B_1 in the middle layer; and C_1 in the bottom layer) within a rectangular container ($30 \times 22 \times 6$ cm^3) placed on the bottom electrode (Fig. 3). These typical positions inside the soybean samples were then used to determine the insect temperature distribution within three layers. Three vertical positions (A_1, B_1, and C_1) in the top, middle, and bottom layers (2, 4, and 6 cm from the bottom of sample) were selected at the center part for each layer where the cold spots were located [29,30]. Therefore, a set of simulations was performed by varying the insect's positions in the container with the insect size of $12H \times 2.5D$ mm^2.

2.5.2. Simulation results with different insect placements

The temperature distributions for horizontally or vertically placed samples were different between the fixed RF electrodes [25,41,42]. So the insect body placement in the rectangular soybeans container may influence the electric field distribution within the insect body [13]. To determine the temperature profiles of insect larvae at each placement, a series of simulations were run by changing the patterns of insect placements (vertical, oblique with 45°, and horizontal in cross-section of x–z) at the top surface center of soybean samples with the same cylinder shape (Fig. 4).

2.5.3. Simulation results with different insect dielectric properties

Dielectric properties of the insect may change with insect species, developmental stages of those species, ages of the insect, and components at a constant temperature, which would influence the RF heating behavior. Dielectric properties of Indianmeal moth, coding moth, and cowpea weevil in different temperature have been measured before (Fig. 5). Dielectric constant and loss factor of insects increased linearly with increasing temperature from 20 to 60 °C. To investigate the effect of dielectric properties on insect temperature rising during RF heating, three different regression models were developed. Temperature distributions of insects with three given dielectric properties were evaluated through the validated simulation model.

2.5.4. Simulation results with different insect sizes

The final insect temperature or heating rate after RF heating could also be influenced by its size according to the energy absorption and heat transfer with the host products. To evaluate the influence of various insect sizes on the RF heating rate, four additional sizes ($10H \times 2.8D$ mm^2, $11H \times 2.6D$ mm^2, $12H \times 2.4D$ mm^2, $13H \times 2.2D$ mm^2, respectively) of cylinder-shaped insects placed at the top surface center of soybeans were assessed using the simulation model together with the originally given size (Fig. 6). Trends of the insect temperature change with four different sizes were determined in each simulation.

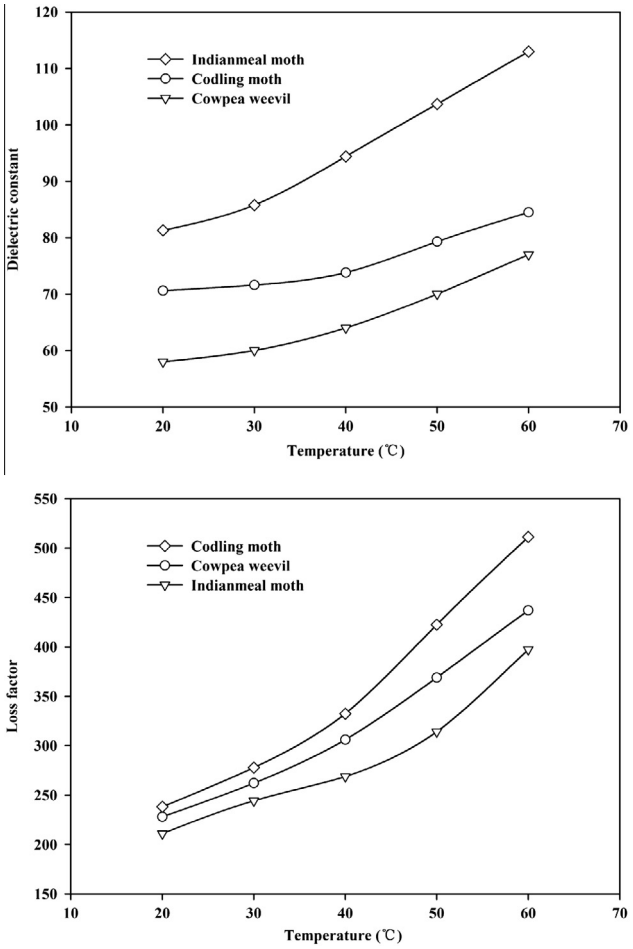

Fig. 5. Dielectric constant and Loss factor for three different insects at temperature range of 20–60 °C and frequency of 27.12 MHz [11,12].

3. Results and discussion

3.1. Model development and validation

Fig. 7 shows a comparison between experimental and simulated surface temperature contours of soybeans in three selected layers within the soybean samples. Results demonstrated that the simulated and experimental temperature distribution patterns for all three layers were in good agreement. Values of the experimentally determined temperature and the simulated one matched well except for corners of the sample where simulated temperature

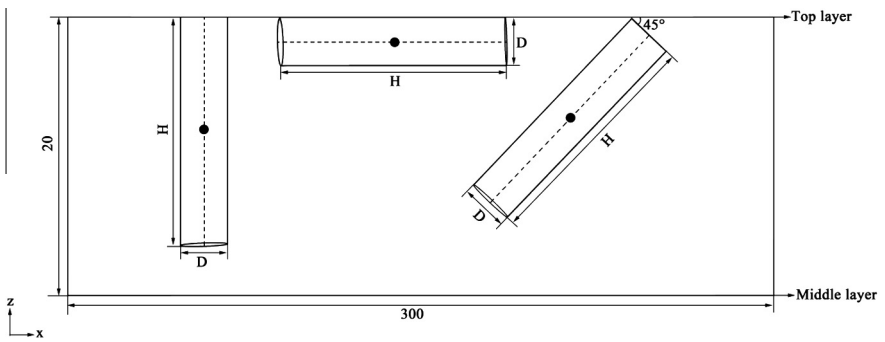

Fig. 4. Different placements (vertical, oblique and horizontal in cross-section of x–z) of insects at the top surface center of dry soybeans with electrode gap of 12 cm, simulated RF heating time of 6 min, and initial temperature of 25 °C (all dimensions are in mm).

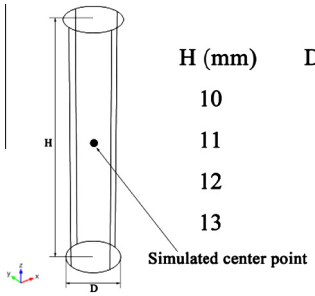

H (mm)	D (mm)	Size (mm²)
10	2.8	10H×2.8D
11	2.6	11H×2.6D
12	2.4	12H×2.4D
13	2.2	13H×2.2D

Fig. 6. Different sizes of insects placed at the top surface center of dry soybeans with insect body positioned vertically, electrode gap adjusted to 12 cm, and initial temperature of 25 °C.

was found to be higher than that determined by experiments. Differences between simulation and experiment could be caused by the ignored moisture migration from outer hot sections to inner cold sections in simulation and the measurement errors for model parameters [24,29,30]. Corners heating were obviously observed for all layers and cold spots were found at the center part for each layer. Electrical field concentrated at corners and edges of the sample was caused by the electrical field refraction and reflection, resulting in higher temperature distributions on these parts [29].

Temperature–time histories of soybeans and cylinder-shaped insects ($12H \times 2.5D$ mm^2) at the center of each layer (1.4, 3.4, and 5.4 cm from the container bottom) were also compared (Fig. 8). Simulated and experimental temperature–time histories of soybeans and cylinder-shaped insects measured at these parts (1, 2, 3 and 4, 5, 6) were also in good agreement (Fig. 2). A similar heating rate of 4.17 and 5.52 °C/min for soybeans and insects in each layer was obtained between simulation and experiment over the heating period. Table 2 compares simulated and experimental average and standard deviation of temperatures for soybeans and insects in three horizontal layers after 6 min RF heating. The experimental average temperatures matched well with the simulated ones, while the simulated standard deviations in each layer were higher. This may be due to the finer mesh of corners and edges than those in central parts of soybean samples in the model (Fig. 7) while those are distributed equally in the experiment.

When soybeans were heated at 27.12 MHz from 25 to 50 °C, the maximum heating rate of vertical insects was 5.83 °C/min, which was greater than that of soybeans (4.17 °C/min) during the same RF treatment. The temperature difference between soybeans and insects in the top, middle, and bottom layers were about 5.9, 6.6, and 6.2 °C, respectively. These values corresponded to a heating rate for the insect of 1.4 times greater than that for soybeans. The similar differential heating results have been obtained for insects in walnut and almond kernels during RF treatments [13,18]. The relative RF heating rate for insect-to-wheat varied between 0.89 and 1.33 [19]. Slightly preferential heating of insects in soybeans using RF energy may have potential benefits in heating the insect to their lethal temperature selectively, while keeping the host products at moderate temperatures.

3.2. Effect of insect position

Fig. 9(a) and (b) present the simulated temperature–time histories at the geometric center of cylinder-shaped insects located in the center surface of three horizontal layers (A_1, B_1, and C_1) and three locations of the top surface layer (A_1, A_2, and A_3) after 6 min RF heating (Fig. 3). In three horizontal positions at the top surface layer of samples, the heating rate in center part (A_1) was lower than corner and edge (A_2, A_3) of samples under the same

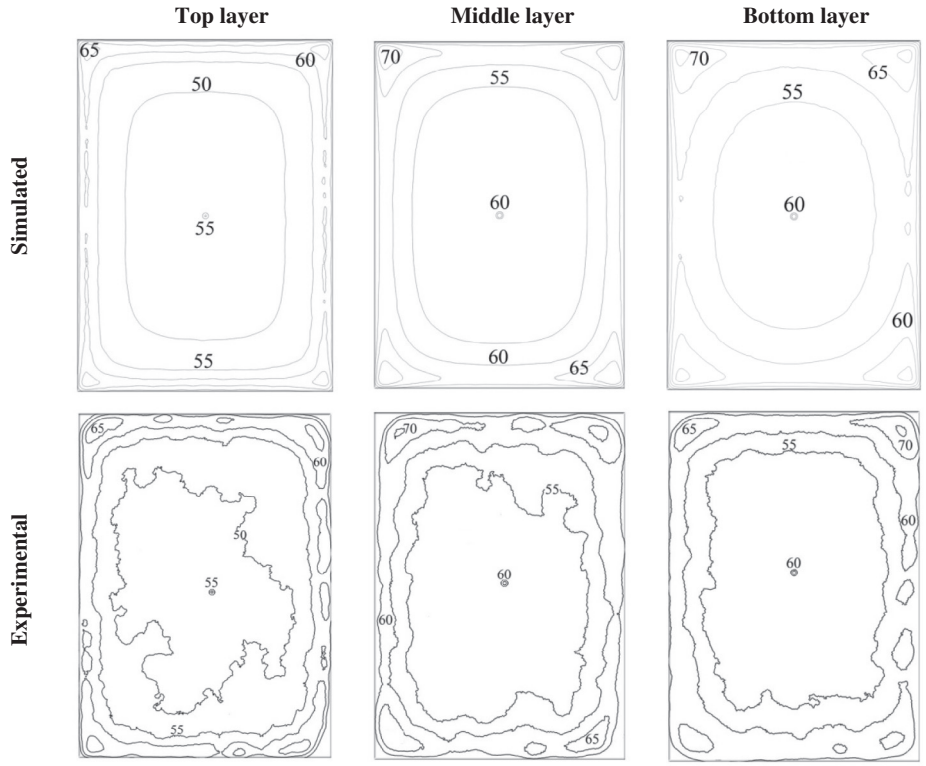

Fig. 7. Comparison of simulated and experimental temperatures for top, middle, and bottom layers of dry soybeans and three insects at the geometric center of each layers (2, 4, and 6 cm from the bottom of sample), placed in a polypropylene container ($30 \times 22 \times 6$ cm^3) on the ground electrode with insect body positioned vertically under the same RF heating conditions.

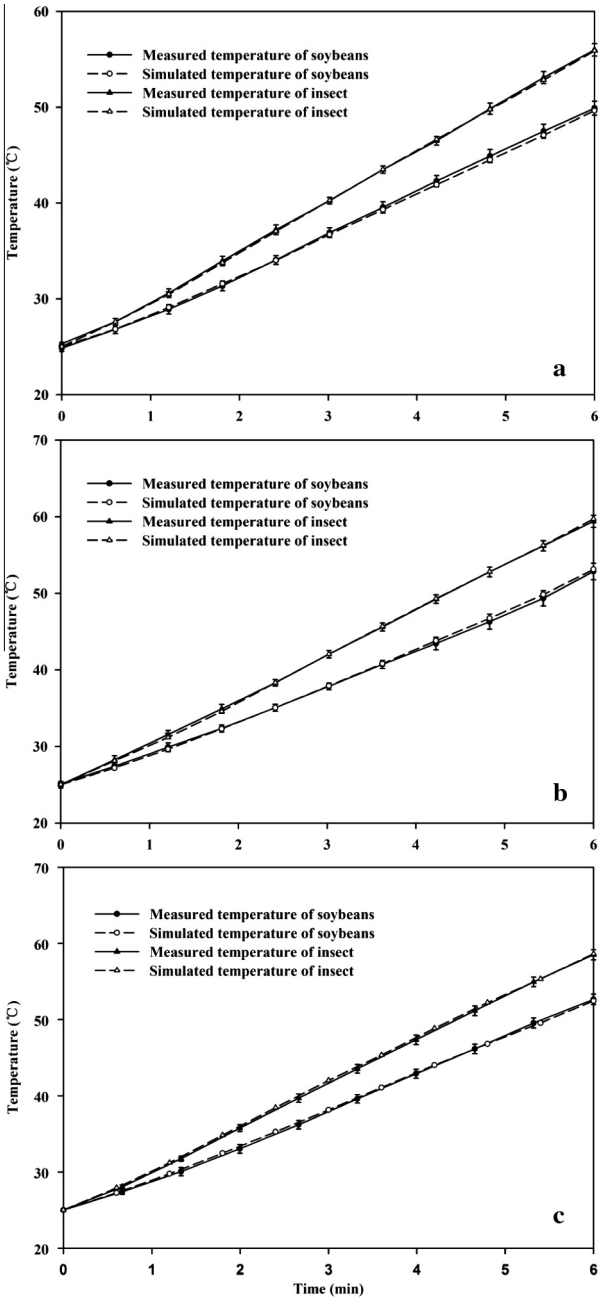

Fig. 8. Validation of the computer simulation results by comparing experimental data with simulated temperature–time histories of dry soybeans and insects at the center part (1.4, 3.4, and 5.4 cm from the bottom of container) of top (a), middle (b), and bottom layers (c) of samples under the same RF heating conditions.

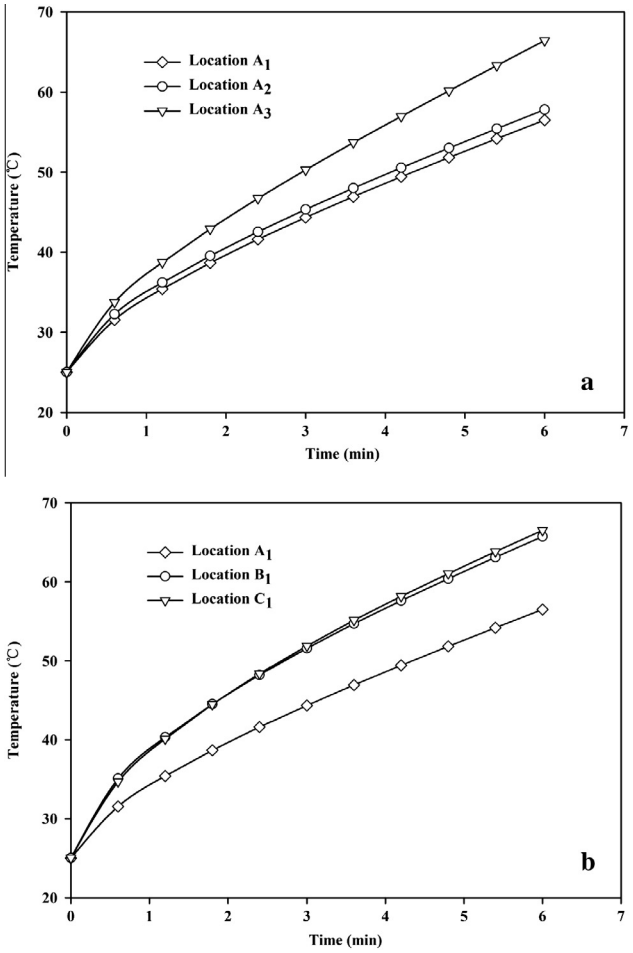

Fig. 9. Computer simulated temperature profiles at the geometric center of insects located at each positions in the top surface layer (A_1, A_2, and A_3) (a) and center part of three horizontal layers (A_1, B_1, and C_1) (b) with insect body positioned vertically under the same RF heating conditions.

Table 2
Comparison between simulated and experimental average (Ave) and standard deviation (SD) temperatures (°C) of dry soybeans at three horizontal layers after 6 min RF heating at a fixed electrode gap of 12 cm and initial temperature of 25 °C.

Layer	Simulated		Experimental	
	Ave	SD	Ave	SD
Top	53.77	4.90	53.39	4.93
Middle	57.94	5.28	56.14	5.24
Bottom	56.22	5.96	55.43	5.83

Table 3
Simulated average (Ave), maximum (Max) and minimum (Min) temperatures (°C) of insects over the volume at nine different locations within the soybeans.

Layer		Min	Max	Max–Min	Ave
Top layer	A_1	55.32	59.87	4.55	57.71
	A_2	55.14	61.60	6.46	58.04
	A_3	61.23	72.12	10.89	66.00
Middle layer	B_1	63.41	65.67	2.26	64.83
Bottom layer	C_1	64.85	68.33	3.48	66.40

RF processing conditions (Fig. 9(a)). This heating behavior was similar to that of treated soybeans at the same position, which was probably caused by the deflected electrical field at corners and edges of soybean samples. In three vertical positions (A_1, B_1, and C_1) in top, middle, and bottom layers of soybeans, the final temperature of insect was the highest in the bottom layer of soybeans and followed by the middle and top layers (Fig. 9(b)). This may be caused by the increased electric field concentration at the contact surfaces when the container was placed on the bottom electrode.

Table 3 compares the simulated average temperatures of insects over the volume at five different locations in three horizontal layers, which was in good agreement with Fig. 9. That is, the higher temperature values of insects were appeared at the positions of corners, edges, and lower sections of the sample. As a result, variation in insect positions caused a relatively large variation in insect heating rate. When insects were placed on the top

layer center of dry soybeans, the temperature values were the lowest. It is, therefore, possible to optimize the reasonable RF treatment time and heating conditions based on the final temperature of food material at the center part of each layer to obtain the adequate control of insects. These findings are corroborated by edges and lower sections overheating of model fruit, and cylindrical meat batters placed on the bottom electrode [25,27]. Similar heating patterns were reported in walnuts [43], polyurethane foam sheets [44], wheat flour [30] and dry fruit [29] subjected to RF treatment.

3.3. Influence of insect placement

Figs. 10 and 11 summarize the effect of insect placements (vertical, oblique and horizontal) on temperature and electric field distribution along the center cross-sectional using the simulation model. Simulated results in Fig. 10 illustrate that the temperature values were higher at low part of the insect when it was placed vertically or obliquely, while lower temperature values were observed with horizontal placement. Simulated results also demonstrated how electric field patterns between two RF electrodes were distributed in the presence of the cylinder-shaped insect with three different placements (Fig. 11). Electric field was the lowest when the cylinder-shaped insect was placed horizontally within soybeans. RF power density at any insect placement is proportional to the square of electric field, resulting in corresponding temperature values at these parts [30]. So patterns of the insect temperature distribution were similar to the electric field. For a given frequency, an increase in field intensity increases the heating rate of insects and high electric field intensities were much more efficient than low intensities in killing insects in products [45]. The vertically and obliquely placed insects were expected to heat more energy as the electric field varied from 473 to 64,800 V/m, and 812 to 42,051 V/m as compared with 100 to 24,673 V/m for the horizontal placement.

Different distribution of electric field within the insect body could be further explained by the vertically distributed electric field between two electrodes. Dielectric materials within the electromagnetic field were heated based on the rapid oscillation of the electric field, causing the charged ions to move back and forth at high speed, and the polar molecules to rotate rapidly. This molecular motion may generate more heat when the insect was placed vertically or obliquely due to the long migration path for polar molecules in the vertical direction [28]. The average temperature was higher for vertically placed insect, and the horizontally and obliquely placed insects were almost with similar average temperature (Table 4).

Fig. 12 shows the simulated temperature–time history of cylinder-shaped insects with different placements after 6 min RF heating. The results demonstrated that the heating rate for vertically placed insect was much higher than that obliquely and horizontally placed insects. The heating rate of horizontally placed insect (4.30 °C/min) was almost similar to that of the soybean samples (4.19 °C/min). The similarity of the heating in soybeans and insects was also depending on the gap between the electrodes [46]. Similar findings have been reported for the typical temperature–time history of horizontally and vertically oriented walnuts in the center of a single layer that temperatures of vertically oriented walnuts were 7.4 °C higher than those of horizontally

Table 4
Simulated average (Ave), maximum (Max) and minimum (Min) temperatures (°C) of insects over the volume with three different placements (vertical, oblique and horizontal) located at the top surface center of soybeans.

Placement	Min	Max	Max–Min	Ave
Vertical	55.32	59.87	4.55	57.71
Oblique	52.10	56.38	4.28	53.70
Horizontal	51.42	52.48	1.06	51.65

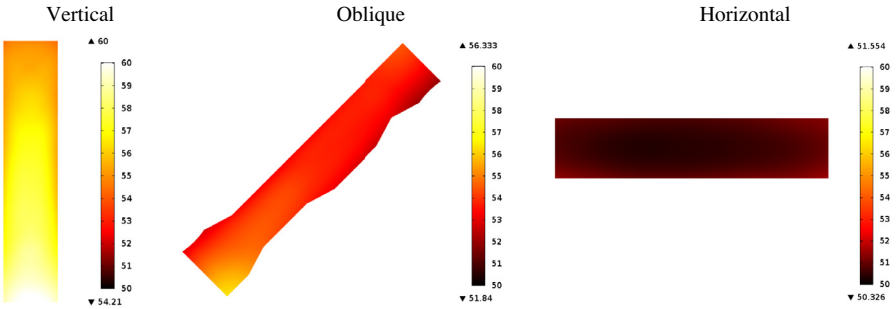

Fig. 10. Computer simulated temperature (°C) distribution of insects ($12H \times 2.5D$ mm^2) along the central cross-sectional with three different placements (vertical, oblique and horizontal) located at the top surface center of soybeans under the same RF heating conditions.

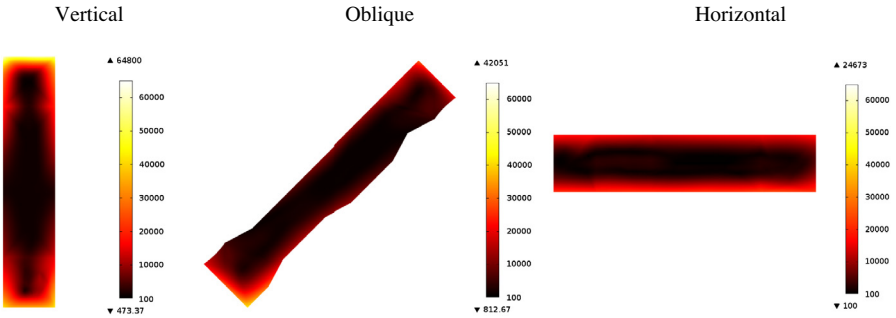

Fig. 11. Simulated electric field (V/m) distribution of insects ($12H \times 2.5D$ mm^2) along the central cross-sectional with three different placements (vertical, oblique and horizontal) located at the top surface center of soybeans under the same RF heating conditions.

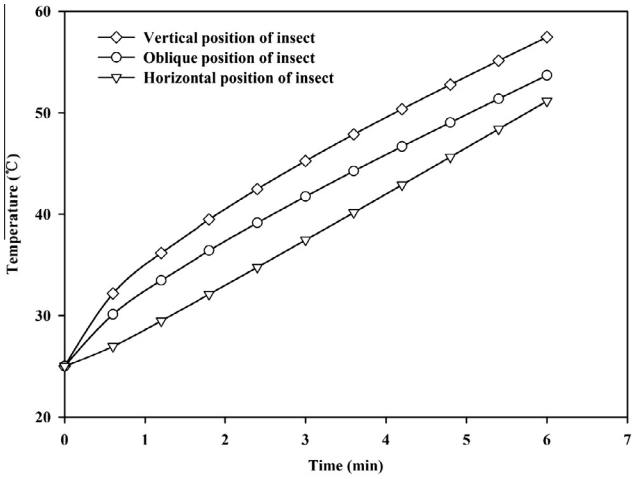

Fig. 12. Computer simulated temperature–time histories at the geometric center of insects located at the top surface center of soybeans with three different placements (vertical, oblique and horizontal) under the same RF heating conditions.

oriented walnuts after 5 min of RF heating [41]. The surface temperature profiles of polyurethane foam sheets were also different for horizontal or vertical placement [42]. Considering the influence of insect placement, the target temperature and heating time based on the thermal death kinetics should be obtained before treatment with RF energy. Temperature of the host product could be heated less than that of insects due to possible differential heating during RF treatments.

3.4. Effect of insect dielectric properties

Fig. 13 shows the simulated temperature–time histories at the geometric center of cylinder-shaped insects influenced by both the dielectric constant and loss factor. During 6 min RF heating, the heating rate was higher both for Indianmeal moth and cowpea weevil, while the coding moth was heated slowly. The maximum, minimum, and average temperatures of insects with different dielectric properties are summarized in Table 5. Although loss factors of Indianmeal moth were the lowest and dielectric constants were the highest among three insects, the average temperature of Indianmeal moth was the highest (Table 5).

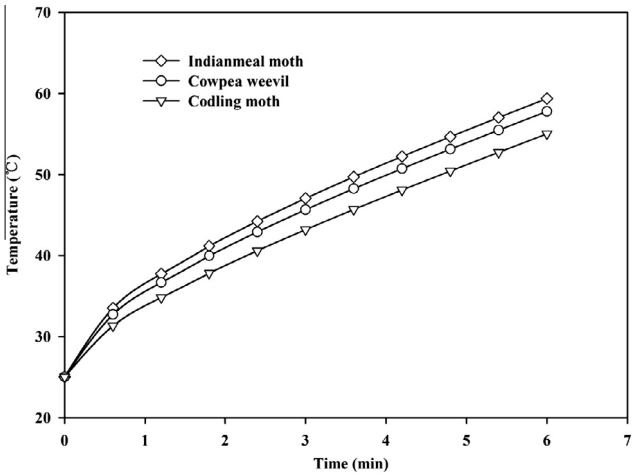

Fig. 13. Computer simulated temperature–time histories at the geometric center of insects located at the top surface center of soybeans with three different dielectric properties and insect body positioned vertically under the same RF heating conditions.

As shown in Fig. 5, values of ε' and ε'' increased almost linearly with temperature (20–60 °C) at a constant frequency. There was a significant difference between ε of Indianmeal moth ($\varepsilon' = 83.37$, $\varepsilon'' = 220.3$) and that of bulk soybeans ($\varepsilon' = 2.01$, $\varepsilon'' = 0.12$) at 25 °C and 27.12 MHz. The relative complex permittivity (ε) for insects and host soybeans was expressed by the regression equation developed in Table 1. Therefore, the magnitudes of ε were considered for both soybeans and insects to estimate E_i from Eq. (7), and to calculate E_{is} using Eq. (8). The electric field intensity in insects decreased with the increase of the relative complex permittivity of the insect (ε_i) as shown in Eq. (7). For higher loss factor materials ($\varepsilon''/\varepsilon' \gg 1$), ε'' increased faster than ε' as the temperature increased, so ε can be substituted by ε'' in Eq. (7) with a negligible error in ε'. This theoretical model discussed above may help for better understand the simulation results that the average temperature decreased with the increase of insect loss factors as shown in Table 5. An analysis of the data, based on relationships presented in Eqs. (7) and (8), reveals that the loss factor is the dominant factor influencing differential energy absorption from the RF field. Similar results have been reported for significant preferential heating of insects in stored-grain, depending mainly on the dielectric properties of insects and characteristics of the host materials [13,19,45]. Therefore, knowledge of dielectric properties of insects and products would yield useful information for future studies on modeling the improvement and scaling-up of RF treatment protocols.

3.5. Effect of insect size

The effect of insect sizes on temperature–time history at the geometric center when subjected to 6 min RF heating was assessed using the simulation model (Fig. 14). Simulated results demonstrated that the center temperature of insects took about 5.8, 4.9, 4.1 and 3.2 min to reach 50 °C for sizes of $10H \times 2.8D$, $11H \times 2.6D$, $12H \times 2.4D$, and $13H \times 2.2D$ mm^2, respectively. The heating process for small diameter insect was much faster than large insect as shown in Eq. (6)[13,32]. The temperature increased slowly for the short and fat insect, but small insects were much easy to be killed during RF heating due to relatively fast heating. Simulated average temperature was the highest with insect sizes of $13H \times 2.2D$ (Table 6). It is clear from Fig. 14 and Table 6 that the temperature of insects was higher than soybeans with various insect sizes. Similar heating patterns have been observed for different sized fruit [25], and wheat flour [22] when subjected to RF treatments.

3.6. General applications of simulation results

To investigate the feasibility of RF selective heating for disinfesting legumes, a computer simulation model was developed in this study to predict transient temperature profiles both in insect bodies and soybean samples. Simulation results of insects and soybeans were validated by experimental temperature profiles over three layers in a rectangular container. The differential heating between insects and treated products may result in increased insect temperatures at relatively low product ones [13,19]. An analysis of the model parameters was proposed to predict their effects on the temperature difference between insect and host product during RF heating. The quantitative data should be regarded only as relative indications, because simplistic but realistic assumptions were made in the simulation model. However, these results alone could provide useful guidance for further research on heat disinfestations of various insects in legumes or other products [6,14,18]. This preferential heating study would be served as a first step to study the feasibility of scaling up the pilot-scale RF system to commercial applications.

Table 5
Simulated average (Ave), maximum (Max) and minimum (Min) temperatures (°C) of insects over the volume with three different dielectric properties located at the top surface center of soybeans.

Material	Dielectric properties	Min	Max	Max–Min	Ave
Indianmeal moth	$(0.81 * T + 63.12) - j(4.42 * T + 109.86)$	55.32	59.87	4.55	57.71
Cowpea weevil	$(0.48 * T + 46.60) - j(5.25 * T + 110.40)$	54.55	59.26	4.71	56.58
Coding moth	$(0.35 * T + 61.76) - j(6.91 * T + 79.98)$	52.97	58.12	5.15	53.00

T-temperature ($20 \leqslant T \leqslant 60$ °C).

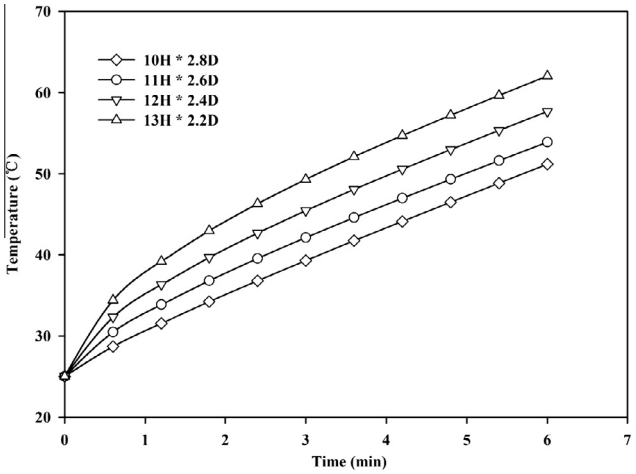

Fig. 14. Computer simulated temperature–time histories at the geometric center of insects located in the top surface center of dry soybeans with four different sizes and insect body positioned vertically under the same RF heating conditions.

Table 6
Simulated average (Ave), maximum (Max) and minimum (Min) temperatures (°C) of insects over the volume with four different sizes located at the top surface center of soybeans.

Size (mm^2)	Min	Max	Max–Min	Ave
$10H \times 2.8D$	51.38	55.20	3.82	52.77
$11H \times 2.6D$	53.47	57.56	4.09	54.77
$12H \times 2.4D$	56.57	60.28	3.71	58.18
$13H \times 2.2D$	62.23	64.00	1.77	62.23

4. Conclusions

A computer simulation model was developed for RF dielectric heating of Indianmeal moth larvae in dry soybeans to investigate the feasibility of selective heating in a 6 kW, 27.12 MHz RF system. Results from computer simulation and experimental methods showed good agreement for the temperature distribution in three horizontal layers of soybeans packed in a plastic container. Simulated and experimental results both showed that cold spots were located at the center part of each layer. The mean temperature differences between insects and soybeans at the top, middle, and bottom layers were 5.9, 6.6, and 6.2 °C, respectively. The validated simulation model was further used to study the effects of insect positions, insect placements, insect dielectric properties, and insect sizes on the behavior of RF preferential heating. Simulated results showed that when the insect was placed on the top surface center, horizontally placed in the host medium, and large insect size would cause relatively slow heating rate as well as low average temperature. The developed simulation model can help designing the practical treatment protocol to maintain selective RF heating and achieve the optimum product temperatures for completely controlling the insect without adverse effects on host product quality.

Conflict of interest

None declared.

Acknowledgments

This research was conducted in the College of Mechanical and Electronic Engineering, Northwest A&F University, and supported by research grants from Ph.D. Programs Foundation of Ministry of Education of China (20120204110022) and General Program of National Natural Science Foundation of China (No. 31371853). The authors thank Qian Hao, Hankun Zhu, and Rongjun Yan for their helps in conducting experiments.

References

[1] FAOSTAT, The agricultural trade domain, exports/countries by commodity, 2011. Available at <http://faostat.fao.org/site/342/default.aspx>.
[2] P.K. Ghosh, D.S. Jayas, Storage of Soybean, The Soybean: Botany, Production and Uses, 2010.
[3] S. Wang, J. Tang, Radio frequency and microwave alternative treatments for insect control in nuts: a review, Agric. Eng. J. 10 (3) (2001) 105–120.
[4] M. Gao, J. Tang, Y. Wang, J. Powers, S. Wang, Almond quality as influenced by radio frequency heat treatments for disinfestation, Postharvest Biol. Technol. 58 (3) (2010) 225–231.
[5] F. Marra, L. Zhang, J.G. Lyng, Radio frequency treatment of foods: review of recent advances, J. Food Eng. 91 (4) (2009) 497–508.
[6] S. Jiao, J. Johnson, J. Tang, S. Wang, Industrial-scale radio frequency treatments for insect control in lentils, J. Stored Prod. Res. 48 (2012) 143–148.
[7] S. Wang, G. Tiwari, S. Jiao, J. Johnson, J. Tang, Developing postharvest disinfestation treatments for legumes using radio frequency energy, Biosyst. Eng. 105 (3) (2010) 341–349.
[8] M.R. Hossan, P. Dutta, Effects of temperature dependent properties in electromagnetic heating, Int. J. Heat Mass Transfer 55 (13) (2012) 3412–3422.
[9] W. Guo, G. Tiwari, J. Tang, S. Wang, Frequency, moisture and temperature-dependent dielectric properties of chickpea flour, Biosyst. Eng. 101 (2) (2008) 217–224.
[10] W. Guo, S. Wang, G. Tiwari, J.A. Johnson, J. Tang, Temperature and moisture dependent dielectric properties of legume flour associated with dielectric heating, LWT-Food Sci. Technol. 43 (2) (2010) 193–201.
[11] S. Jiao, J. Johnson, J. Tang, G. Tiwari, S. Wang, Dielectric properties of cowpea weevil, black-eyed peas and mung beans with respect to the development of radio frequency heat treatments, Biosyst. Eng. 108 (3) (2011) 280–291.
[12] S. Wang, J. Tang, J. Johnson, E. Mitcham, J. Hansen, G. Hallman, S. Drake, Y. Wang, Dielectric properties of fruits and insect pests as related to radio frequency and microwave treatments, Biosyst. Eng. 85 (2) (2003) 201–212.
[13] S. Wang, J. Tang, R. Cavalieri, D. Davis, Differential heating of insects in dried nuts and fruits associated with radio frequency and microwave treatments, Trans. ASAE 46 (4) (2003) 1175–1184.
[14] M. Lagunas-Solar, Z. Pan, N. Zeng, T. Truong, R. Khir, K. Amaratunga, Application of radiofrequency power for non-chemical disinfestation of rough rice with full retention of quality attributes, Appl. Eng. Agric. 23 (5) (2007) 647–654.
[15] E. Mitcham, R. Veltman, X. Feng, E. Castro, J. Johnson, T. Simpson, W. Biasi, S. Wang, J. Tang, Application of radio frequency treatments to control insects in in-shell walnuts, Postharvest Biol. Technol. 33 (1) (2004) 93–100.
[16] S. Wang, M. Monzon, J. Johnson, E. Mitcham, J. Tang, Industrial-scale radio frequency treatments for insect control in walnuts: II: Insect mortality and product quality, Postharvest Biol. Technol. 45 (2) (2007) 247–253.
[17] S. Nelson, L. Charity, Frequency dependence of energy absorption by insects and grain in electric fields, Trans. ASAE 27 (1972) 1099–1102.
[18] S. Wang, J. Tang, J. Johnson, R. Cavalieri, Heating uniformity and differential heating of insects in almonds associated with radio frequency energy, J. Stored Prod. Res. 55 (2013) 15–20.
[19] B. Shrestha, O.D. Baik, Radio frequency selective heating of stored-grain insects at 27.12 MHz: a feasibility study, Biosyst. Eng. 114 (3) (2013) 195–204.

[20] C.J. Budd, A.D.C. Hill, A comparison of models and methods for simulating the microwave heating of moist foodstuffs, Int. J. Heat Mass Transfer 54 (2011) 807–817.
[21] V. Romano, F. Marra, A numerical analysis of radio frequency heating of regular shaped foodstuff, J. Food Eng. 84 (3) (2008) 449–457.
[22] G. Tiwari, S. Wang, J. Tang, S. Birla, Analysis of radio frequency (RF) power distribution in dry food materials, J. Food Eng. 104 (4) (2011) 548–556.
[23] M.R. Hossan, D.Y. Byun, P. Dutta, Analysis of microwave heating for cylindrical shaped objects, Int. J. Heat Mass Transfer 53 (2010) 5129–5138.
[24] Z. Huang, H. Zhu, R. Yan, S. Wang, Simulation and prediction of radio frequency heating in dry soybeans, Biosyst. Eng. 129 (2) (2015) 34–47.
[25] S. Birla, S. Wang, J. Tang, Computer simulation of radio frequency heating of model fruit immersed in water, J. Food Eng. 84 (2) (2008) 270–280.
[26] J. Wang, R.G. Olsen, J. Tang, Z. Tang, Influence of mashed potato dielectric properties and circulating water electric conductivity on radio frequency heating at 27 MHz, J. Microw. Power Electromagn. Energy. 42 (2) (2008) 31–46.
[27] F. Marra, J. Lyng, V. Romano, B. McKenna, Radio-frequency heating of foodstuff: solution and validation of a mathematical model, J. Food Eng. 79 (3) (2007) 998–1006.
[28] Y. Jiao, J. Tang, S. Wang, A new strategy to improve heating uniformity of low moisture foods in radio frequency treatment for pathogen control, J. Food Eng. 141 (2014) 128–138.
[29] B. Alfaifi, J. Tang, Y. Jiao, S. Wang, B. Rasco, S. Jiao, S. Sablani, Radio frequency disinfestation treatments for dry fruit: model development and validation, J. Food Eng. 120 (2014) 268–276.
[30] G. Tiwari, S. Wang, J. Tang, S. Birla, Computer simulation model development and validation for radio frequency (RF) heating of dry food materials, J. Food Eng. 105 (1) (2011) 48–55.
[31] H. Zhu, Z. Huang, S. Wang, Experimental and simulated top electrode voltage in free-running oscillator radio frequency systems, J. Electromagn. Waves Appl. 28 (5) (2014) 606–617.
[32] A. Ben-Lalli, P. Bohuon, A. Collignan, J.M. Méot, Modeling heat transfer for disinfestation and control of insects (larvae and eggs) in date fruits, J. Food Eng. 116 (2) (2013) 505–514.
[33] S. Deshpande, S. Bal, T. Ojha, Bulk thermal conductivity and diffusivity of soybean, J. Food Process. Preserv. 20 (3) (1996) 177–189.
[34] S. Deshpande, S. Bal, Specific heat of soybean, J. Food Process Eng 22 (6) (1999) 469–477.
[35] S. Sahin, S.G. Sumnu, Physical Properties of Foods, Springer, New York, 2006.
[36] COMSOL material library, COMSOL Multiphysics, V4.3a, Burlington, MA, USA, 2012.
[37] A.R. von Hippel, Dielectric Materials and Applications, Artech House, Boston, USA, 1995.
[38] A. Metaxas, Foundations of Electroheat: A Unified Approach, Wiley, Chichester, UK, 1996.
[39] J. Johnson, S. Wang, J. Tang, Thermal death kinetics of fifth-instar Plodia interpunctella (Lepidoptera: Pyralidae), J. Econ. Entomol. 96 (2) (2003) 519–524.
[40] J. Johnson, K. Valero, S. Wang, J. Tang, Thermal death kinetics of red flour beetle (Coleoptera: Tenebrionidae), J. Econ. Entomol. 97 (6) (2004) 1868–1873.
[41] S. Wang, J. Tang, T. Sun, E. Mitcham, T. Koral, S. Birla, Considerations in design of commercial radio frequency treatments for postharvest pest control in in-shell walnuts, J. Food Eng. 77 (2) (2006) 304–312.
[42] Y. Wang, L. Zhang, M. Gao, J. Tang, S. Wang, Evaluating radio frequency heating uniformity using polyurethane foams, J. Food Eng. 136 (2014) 28–33.
[43] S. Wang, M. Monzon, J. Johnson, E. Mitcham, J. Tang, Industrial-scale radio frequency treatments for insect control in walnuts: I: Heating uniformity and energy efficiency, Postharvest Biol. Technol. 45 (2) (2007) 240–246.
[44] S. Wang, K. Luechapattanaporn, J. Tang, Experimental methods for evaluating heating uniformity in radio frequency systems, Biosyst. Eng. 100 (1) (2008) 58–65.
[45] S. Nelson, W. Whitney, Radio-frequency electric fields for stored grain insect control, Trans. ASAE 3 (2) (1960) 133–137.
[46] R. Uyar, F. Erdogdu, F. Marra, Effect of load volume on power absorption and temperature evolution during radio-frequency heating of meat cubes: a computational study, Food Bioprod. Process. 92 (2014) 243–251.